

Using a combined PIC-MHD code to simulate particle acceleration in astrophysical shocks

Allard Jan van Marle*

Laboratoire AstroParticule & Cosmologie (APC), Université Paris Diderot, CNRS/IN2P3, CEA/Irfu, Observatoire de Paris, Sorbonne Paris Cité, 10, rue Alice Domon et Leonie Duquet, F-75205 Paris Cedex 13, France
E-mail: vanmarle@apc.in2p3.fr

Fabien Casse

Laboratoire AstroParticule & Cosmologie (APC), Université Paris Diderot, CNRS/IN2P3, CEA/Irfu, Observatoire de Paris, Sorbonne Paris Cité, 10, rue Alice Domon et Leonie Duquet, F-75205 Paris Cedex 13, France
E-mail: fcasse@apc.in2p3.fr

Alexandre Marcowith

Laboratoire Univers et Particules de Montpellier (LUPM) Université Montpellier, CNRS/IN2P3, CC72, place Eugène Bataillon, 34095, Montpellier Cedex 5, France
E-mail: Alexandre.Marcowith@umontpellier.fr

In order to model the magnetic field amplification and particle acceleration that takes place in astrophysical shocks, we need a code that can efficiently model the large-scale structure of the shock, while still taking the kinetic aspect of non-thermal particles into account. Starting from the proven MPI-AMRVAC magnetohydrodynamics code we have created a code that combines the kinetic treatment of the Particle-in-Cell (PIC) method for non-thermal particles with the large-scale efficiency of grid-based hydrodynamics (MHD) to model the thermal plasma, including the use of adaptive mesh refinement. Using this code we simulate astrophysical shocks, varying the angle between the magnetic field and the shock to test our code against existing results and study both the evolution of the shock and the behaviour of non-thermal particles. We find that the combined PIC-MHD method can accurately recover the results that were previously obtained with pure PIC codes. Furthermore, the computational efficiency of the code allows us to explore the available parameter space to a larger degree than has been done in previous work. Our results suggest that efficient particle acceleration can take place in near-oblique shocks where the magnetic field makes a large angle with the direction of the flow.

*35th International Cosmic Ray Conference — ICRC2017
10–20 July, 2017
Bexco, Busan, Korea*

*Speaker.

1. Introduction

Cosmic Rays (CRs) with energies varying between a few GeV to hundreds of PeV are produced through repeated crossings of the charged particles across a shock front that carries magnetic fluctuations, which are responsible for particle scattering [1], a process known as diffusive shock acceleration (DSA). This acceleration process in turn can create turbulence in the magnetic field, which can disturb the shock.

In order to simulate this process numerically, we need a code that is capable of modelling the interactions between charged particles and a magnetic field, but it must also have the ability to model the large scale shock structure. Traditionally, the first is accomplished through the particle-in-cell (PIC) method. This method uses a two-step approach in which the charges and velocities of individual particles are mapped onto a grid to determine charge- and current-density as a function of space. From the charge and current densities the electromagnetic field is computed through the Maxwell's equations. Once computed, the electromagnetic field is then used to move the particles by way of the Lorentz' force and Newton's equation of motion. Unfortunately, while the PIC method is well suited to dealing with the interactions between CRs and an electromagnetic field, it is computationally expensive, which can become prohibitive when dealing with large-scale structures such as astrophysical shocks. The latter can be simulated more quickly through the use of grid-based magnetohydrodynamics (MHD). However, this method relies on representing the gas through average values and includes neither particle physics, nor the ability to simulate a gas that deviates from thermal equilibrium.

Ideally, one would wish to combine these two methods into a single code. A method to accomplish this, based on a rewritten form of Ohm's law was shown by [2] and used by us to produce a code that combines the computational efficiency of grid-based MHD with the ability to simulate the behaviour of non-thermal particles. This is accomplished by splitting the gas into two separate components. The first, which contains the majority of the mass, behaves as a thermal plasma and is simulated with grid-based MHD. The second, which contains those particles that are deviating from the thermal equilibrium, is treated as a collection of individual particles, which are moved through the grid using a Boris-pusher

We use this code to simulate astrophysical shocks that include an existing magnetic field as well as non-thermal particles generated at the shock. The code allows us to simulate a large area in space and follow the behaviour of both the particles and the thermal gas over time.

2. Method

We use the `MPI-AMRVAC` magneto hydrodynamics code [3]. This is a fully conservative finite volume code, which solves the conservation equations of magnetohydrodynamics on an adaptive mesh grid and uses the `OpenMPI` library to allow for parallelization on distributive memory machines. For our adaptation of the code we preserve its existing architecture, including the parallelization and the Octree-based adaptive mesh. In order to account for the presence of charged, supra-thermal particles, we introduce a new form of the conservation equations, following the prescription by [2]

The MHD conservation equations for mass, momentum and energy, including the additional terms that arise from the interaction with the non-thermal particles are:

$$\frac{\partial \rho}{\partial t} + \nabla \cdot (\rho \mathbf{v}) = 0, \quad (2.1)$$

where ρ and \mathbf{v} stand as the mass density and velocity of the thermal plasma,

$$\frac{\partial \rho \mathbf{v}}{\partial t} + \nabla \cdot \left(\rho \mathbf{v} \otimes \mathbf{v} - \frac{\mathbf{B} \otimes \mathbf{B}}{4\pi} + P_{\text{tot}} \mathbb{1} \right) = -\mathbf{F}_{\text{part}}, \quad (2.2)$$

with \mathbf{B} being the magnetic field while $P_{\text{tot}} = P + B^2/8\pi$ is the total pressure. The force exerted by the particles is defined as

$$\mathbf{F}_{\text{part}} = (1 - R)(\mathbf{E}_0 - \mathbf{E})n_i \quad (2.3)$$

with R the relative density of supra-thermal particles compared to the sum of supra-thermal and thermal particles, n_i the charge density of the thermal ions, \mathbf{E}_0 the electric field generated by the thermal plasma and \mathbf{E} the total electric field. The energy equations reads

$$\frac{\partial e}{\partial t} + \nabla \cdot \left((e + P_{\text{tot}})\mathbf{v} + (\mathbf{E} - \mathbf{E}_0) \times \frac{\mathbf{B}}{4\pi} \right) = -\mathbf{u}_{\text{part}} \cdot \mathbf{F}_{\text{part}} \quad (2.4)$$

with \mathbf{u}_{part} the velocity field of the supra-thermal particles. Finally, the magnetic field is updated according to the Maxwell-Ampere equation,

$$\frac{\partial \mathbf{B}}{\partial t} = c\nabla \times \mathbf{E}. \quad (2.5)$$

This set of equations, combined with the adiabatic equation of state, forms a closed set of conservation equations that can be solved on the grid, using the solvers available in the MPI-AMRVAC code. Doing so gives us the properties of the thermal gas as a function of space and time. An extra benefit to this approach is that we do not need to solve the full set of Maxwell's equations to determine the electromagnetic field. Therefore, unlike PIC codes, we do not have the problem of super-luminal Cherenkov waves appearing in our solution.

Meanwhile, the position and velocity of the particles is updated according to the equation of motion, only taking into account the electromagnetic force, namely

$$\frac{\partial \mathbf{p}_j}{\partial t} = q_j \left(\mathbf{E} + \frac{\mathbf{u}_j}{c} \times \mathbf{B} \right) \quad (2.6)$$

with \mathbf{p}_j , q_j and \mathbf{u}_j the momentum, charge and velocity of particle j . This equation can be solved by using a Boris-pusher, which we have added to the code.

In practice, our code handles the combination of MHD and PIC methods by saving the quantities of the thermal gas, then advancing them one times-step using the conservation equations. Once this is done it uses the saved values of the thermal gas (representing the state of the gas at the start of the timestep) to advance the position and velocity of the supra-thermal particles. From the new position of the particles it calculates average charge and current densities, created by the supra-thermal particles, at the cell centres. Both the thermal gas and the supra-thermal particles have now advanced one timestep and the process repeats itself. The length of each timestep is limited by the Courant-Friedrich-Levy condition.

In order to maintain $\nabla \cdot \mathbf{B} = 0$ we have implemented the constrained transport method by [4].

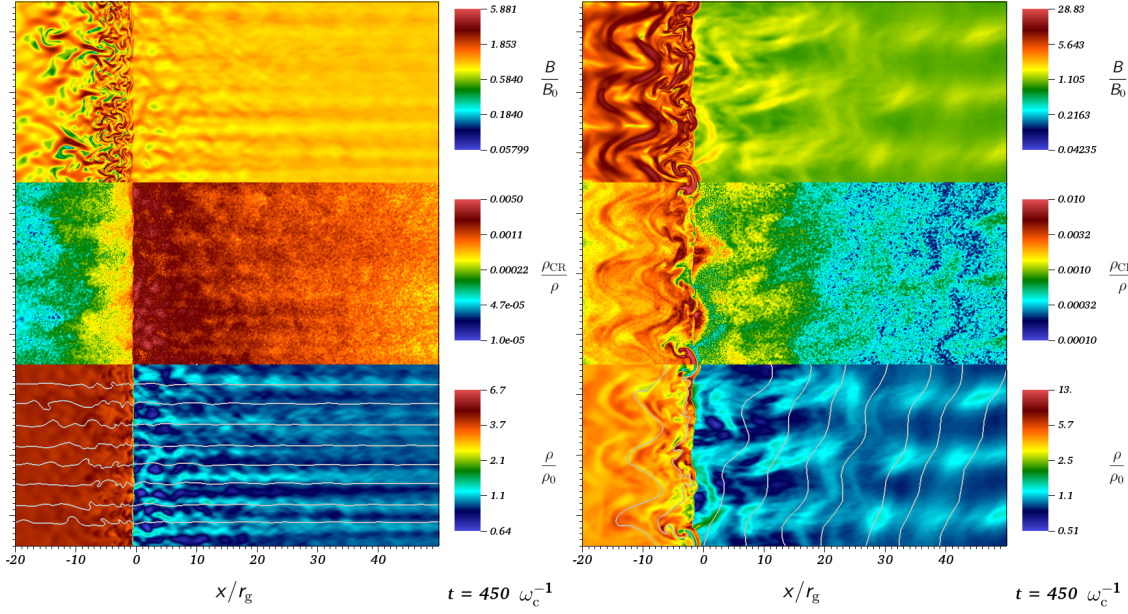


Figure 1: Simulation of a shock with a magnetic field parallel to the flow (left) and with a 70 degree angle between the magnetic field and the flow (right). The shock occurs at $x = 0$, with the fluid moving from right to left in the frame of the shock. Both panels show the condition of the gas after a time of $450 \omega_c^{-1}$. From the top, the magnetic field relative the original upstream field strength, the supra-thermal particle density relative to the thermal gas density, and the thermal gas density relative to the original upstream density.

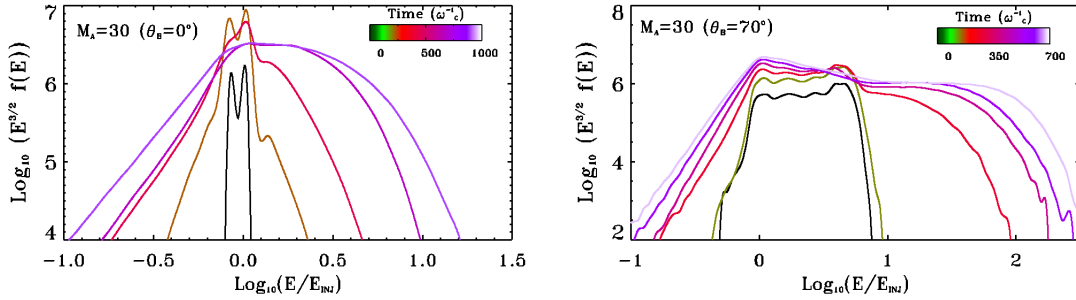


Figure 2: The SED of the particles at various point in time for both the parallel (left) and the near-oblique (right) shock. As time progresses, a plateau appears for particles at higher energies, indicating that Fermi acceleration occurs.

3. Simulations

3.1 The parallel shock case

We test our code by reproducing the simulations shown by [2], which in turn were tested against earlier results obtained with a PIC-hybrid code by [5]. This simulation evolves a shock with Alfvénic Mach number 30 and a magnetic field parallel to the direction of the flow. We use the same resolution as [2] and inject particles at the shock with the same initial velocity, which is equal to three times the pre-shock velocity, and at a rate of 0.002 times the thermal gas density passing through the shock. Unlike [2] we perform the simulation in the rest frame of the shock.

This allows us to use a much smaller physical domain along the axis parallel to the direction of motion.

The result of our calculations is presented on the left side of Fig. 1. On the left we see the state of the gas at a time of $450 \omega_c^{-1}$ with $\omega_c^{-1} = q/mcB_0$ the ion cyclotron frequency, where q and m are the particle charge and mass, c is the speed of light and B_0 is the original upstream magnetic field strength. Here the shock is situated at $x = 0$. The fluid moves from right to left (in the frame of reference of the shock). The axes are measured in gyro radii ($r_g = v_{inj}/\omega_c$ (according to the injection velocity v_{inj} and the original upstream magnetic field strength B_0 .) The three panels show (from top to bottom) the magnetic field strength relative to the initial magnetic field, the supra-thermal particle density relative to the thermal gas density, and the thermal gas density relative to the original upstream density. At this time, the upstream medium (right of the shock) shows a strong filamentary structure (resulting from the non-resonant streaming instability), whereas the downstream medium is highly turbulent. These results coincide with those found in earlier simulations by [2] and [5], as well as confirming the theoretical predictions by [6] and [7]. The left panel of Fig. 2 shows the spectral energy distribution (SED) of the supra-thermal particles in the grid at various moments in time during the simulation. Initially, the energy of the particles remains close to the injection energy (E_{inj}). However, as time progresses, a low energy tail appears (particles that have lost energy to the grid as they initialized the instabilities.) At the same time, some particles are accelerated to higher energies. Over time, the acceleration causes a plateau to appear, which on the scale used here ($E^{3/2}f(E)$ as a function of E) indicates that Fermi acceleration is taking place at the shock.

3.2 The near-oblique shock case

As a second test, we change the angle of the magnetic field with the flow to 70 degrees. Such a simulation was performed using the PIC-hybrid method by [5], who concluded that neither magnetic field amplification, nor particle acceleration occurred.

Our results, presented on the right side of Fig. 1 show a different outcome. Particles inserted near the shock repeatedly cross the shock as they circle around the magnetic field lines. Because the downstream field is stronger than the upstream field, due to the compression, each transition from upstream to downstream increases the particle energy. Eventually, the particles gain enough speed to start moving into the upstream medium, creating an upstream current. Meanwhile, the shock itself becomes corrugated on a long wavelength. Therefore, the magnetic field becomes more oblique in some locations and less oblique in others, creating local current streams, which influence the upstream magnetic field. As a result, a similar long-wavelength variation appears in the upstream medium, which upon encountering the shock increases the corrugation and creates a turbulent down-stream medium. The particle SED, shown in the right panel of Fig. 2 shows that initially there is only a limited spread in particle energies. However, after approximately $t=250 \omega_c^{-1}$, a high energy feature starts to form, which eventually leads to a Fermi plateau, similar to the one found for the parallel shock case.

4. Discussion

Whereas our results for the parallel shock corroborate earlier results, the near-oblique shock

model deviates considerably from the PIC result. We identify a number of factors that contribute to this outcome.

1. We have a larger number supra-thermal particles, because all particles effectively behave in a supra-thermal fashion, unlike a PIC code, where most particles are part of the thermal plasma. A larger number of supra-thermal particles is necessary to obtain the upstream current. The key to this particular issue is the absolute number of particles, rather than the resolution. If the total number of particles is insufficient it is impossible to form an upstream current.
2. Our simulation domain is six times larger along the perpendicular axis than what was used by [5], which allows us to capture the long wavelength. Without this wavelength, the shock corrugation does not occur. As a result, the upstream current will not show significant spatial variation and the upstream magnetic field will remain undisturbed.

Testing our simulations further, we find that we recover the result by [5] if we reduce our physical domain to the same size they used.

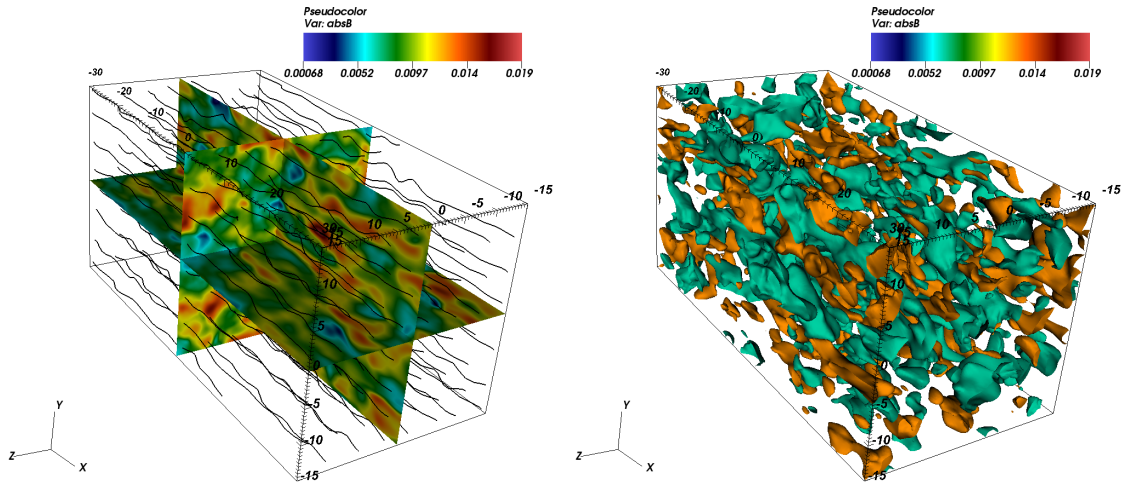


Figure 3: Magnetic field strength and streamlines in the upstream medium. This 3-D simulation shows the formation of streaming instabilities.

5. Conclusions and Outlook

Our initial results for a parallel shock have been successful in reproducing previous simulations that used either PIC or a combine MHD-PIC approach, confirming the viability of the method and our code. However, the near-oblique magnetic field model shows a result that deviates considerably from previous models. We can explain the difference by considering the smaller scale (both in space and time) of the earlier models. This demonstrates the advantage of the combined PIC-MHD approach, which allows for the efficient computation of large-scale simulations.

In the future we intend to repeat these simulations in 3-D, for which the PIC-MHD is uniquely suited thanks to its computational efficiency. As a first demonstration we present a simulation of

the upstream medium in the parallel shock case (Fig. 3), using similar input parameters as it is influenced by the supra-thermal particles that are being created at the shock. On the left we show the magnetic field strength in 3-D slice as well as the magnetic field lines. On the right we present iso-surfaces of the magnetic field strength, showing the complex 3-D structure of the streaming instability. Because this simulation does not include the shock itself it can only reproduce the early stages of the process. Introducing the shock in the 3-D model will be the next step in this investigation

Once we have explored the effect of 3-D simulations, we intend to introduce special relativistic MHD in order to model early supernovae as well as gamma ray bursts and the jets of active galactic nuclei.

Acknowledgments

We are grateful for fruitful regular discussions with: A.R. Bell, C.A. Bret, A. Bykov, M. Dieckmann, E. D’huimières, M. Grech, L. Gremillet, R. Keppens, B. Lembège, M. Lemoine, G. Pelletier, I. Plotnikov, V. Tikhonchuk. This work is supported by the ANR-14-CE33-0019 MACH project.

References

- [1] L. O. Drury, *An introduction to the theory of diffusive shock acceleration of energetic particles in tenuous plasmas*, *Reports on Progress in Physics* **46** (1083) 973
- [2] X.-N. Bai, D. Caprioli, L. Sironi, & L. Spitkovsky, *Magnetohydrodynamic-particle-in-cell Method for Coupling Cosmic Rays with a Thermal Plasma: Application to Non-relativistic Shocks*, *ApJ* **809** (2015) 55
- [3] B. van der Holst, R. Keppens & Z. Meliani, *A multidimensional grid-adaptive relativistic magnetofluid code*, *Comp. Phys. Commun.* **179** (2008) 617
- [4] D. S. Balsara & D. S. Spicer, *A Staggered Mesh Algorithm Using High Order Godunov Fluxes to Ensure Solenoidal Magnetic Fields in Magnetohydrodynamic Simulations*, *JCP* **149** (1999) 270
- [5] D. Caprioli & Spitkovski, A., *Simulations of Ion Acceleration at Non-relativistic Shocks. I. Acceleration Efficiency*, *ApJ* **783** (2014) 91
- [6] A. R. Bell, *Turbulent amplification of magnetic field and diffusive shock acceleration of cosmic rays*, *MNRAS* **353** (2004) 550
- [7] A. R. Bell, *The interaction of cosmic rays and magnetized plasma*, *MNRAS* **358** (2005) 181